




Connectivity at the origins of domain specificity in the cortical face and place networks

Frederik S. Kamps^{a,b} , Cassandra L. Hendrix^a, Patricia A. Brennan^a, and Daniel D. Dilks^{a,1}

^aDepartment of Psychology, Emory University, Atlanta, GA 30322; and ^bDepartment of Brain and Cognitive Sciences, Massachusetts Institute of Technology, Cambridge, MA 02139

Edited by Alfonso Caramazza, Harvard University, Cambridge, MA and accepted by Editorial Board Member Renée Baillargeon January 30, 2020 (received for review July 2, 2019)

It is well established that the adult brain contains a mosaic of domain-specific networks. But how do these domain-specific networks develop? Here we tested the hypothesis that the brain comes prewired with connections that precede the development of domain-specific function. Using resting-state fMRI in the youngest sample of newborn humans tested to date, we indeed found that cortical networks that will later develop strong face selectivity (including the “proto” occipital face area and fusiform face area) and scene selectivity (including the “proto” parahippocampal place area and retrosplenial complex) by adulthood, already show domain-specific patterns of functional connectivity as early as 27 d of age (beginning as early as 6 d of age). Furthermore, we asked how these networks are functionally connected to early visual cortex and found that the proto face network shows biased functional connectivity with foveal V1, while the proto scene network shows biased functional connectivity with peripheral V1. Given that faces are almost always experienced at the fovea, while scenes always extend across the entire periphery, these differential inputs may serve to facilitate domain-specific processing in each network after that function develops, or even guide the development of domain-specific function in each network in the first place. Taken together, these findings reveal domain-specific and eccentricity-biased connectivity in the earliest days of life, placing new constraints on our understanding of the origins of domain-specific cortical networks.

development | fMRI | fusiform face area | parahippocampal place area | neonates

Decades of research have uncovered a striking organization of the adult brain wherein many cognitive functions are implemented in domain-specific networks (or sets of cortical regions) specialized for particular tasks, such as recognizing faces or scenes (1). How does this organization emerge? Does the brain begin as a relatively undifferentiated, general-purpose machine, with domain-specific networks emerging only after substantial experience with the world? Or does the brain come prewired with domain-specific patterns of connections already in place, even before those networks are fully functional? Here we address these questions by considering the test cases of the cortical face and scene processing networks, two networks in the ventral visual cortex that are perhaps the most extensively studied domain-specific networks in adults. Using resting-state fMRI (rsfMRI) in the youngest sample tested to date, we find that cortical regions that will later develop face selectivity, including the proto-occipital face area (OFA) and fusiform face area (FFA) (2, 3), and place selectivity, including the proto parahippocampal place area (PPA) and retrosplenial complex (RSC) similar to adults, already show domain-specific patterns of functional connectivity as early as 27 d of age.

The connection between the OFA and FFA in the adult brain is well established. In particular, 1) diffusion tensor imaging (DTI) studies have revealed direct anatomic projections between the OFA and FFA (4, 5); 2) resting state fMRI studies have revealed a functional connection between the OFA and FFA (6, 7), most likely reflecting the anatomic connection reported in the

foregoing DTI findings, and have shown that this functional connection is behaviorally relevant (8); and 3) combined transcranial magnetic stimulation-fMRI studies have found that disruption of the OFA leads to disruption of activation in the FFA, providing causal evidence of this connection (9). Similarly, the connection between the PPA and RSC is well established, with DTI studies revealing direct anatomic projections between the PPA and RSC (4, 5) and rsfMRI studies revealing a functional connection between the PPA and RSC.

While domain-specific patterns of connectivity are thought to have functional significance even in adulthood (8, 10), the discovery of these connections in adults has also led to the hypothesis that connectivity plays a critical role in development (e.g., by ensuring that connected regions will later develop similar domain-specific functions) (10–15). Critically, however, there is limited empirical evidence for such proposals, and the developmental origins of OFA-FFA and PPA-RSC connectivity in infancy have never been explored. Thus, to address this question, we measured functional connectivity between OFA, FFA, PPA, and RSC in the earliest stages of postnatal development, before substantial experience with faces and scenes.

Along with exploring the developmental origins of OFA-FFA and PPA-RSC connectivity, we further asked how these networks are functionally connected with the early visual cortex. It is well established that by adulthood, the face and scene networks show

Significance

Where does knowledge come from? We addressed this classic question using the test cases of the cortical face and scene networks: two well-studied examples of specialized “knowledge” systems in the adult brain. We found that neonates already show domain-specific patterns of functional connectivity between regions that will later develop full-blown face and scene selectivity. Furthermore, the proto face network showed stronger functional connectivity with foveal than with peripheral primary visual cortex, while the proto scene network showed the opposite pattern, revealing that these networks already receive differential visual inputs. Our findings support the hypothesis that innate connectivity precedes the emergence of domain-specific function in cortex, shedding new light on the age-old question of the origins of human knowledge.

Author contributions: F.S.K. and D.D.D. designed research; F.S.K. and C.L.H. performed research; F.S.K., C.L.H., and D.D.D. analyzed data; and F.S.K., C.L.H., P.A.B., and D.D.D. wrote the paper.

The authors declare no competing interest.

This article is a PNAS Direct Submission. A.C. is a guest editor invited by the Editorial Board.

Published under the PNAS license.

Data deposition: The datasets generated during this study are available at the Open Science Framework, <https://osf.io/kmxv7/>.

¹To whom correspondence may be addressed. Email: dilks@emory.edu.

This article contains supporting information online at <https://www.pnas.org/lookup/suppl/doi:10.1073/pnas.1911359117/-DCSupplemental>.

First published March 2, 2020.

distinct retinotopic biases, with the face network biased toward foveal stimulation and the scene network biased toward peripheral stimulation (16–18). Given that faces are typically foveated while scenes inherently extend across the entire visual field, these biased inputs are thought to facilitate domain-specific function in each network; for example, faces may be processed faster or more accurately when presented to the fovea, while scenes may be processed faster or more accurately when presented to the periphery (16, 19, 20). Moreover, beyond this functional significance in adulthood, it also has been hypothesized that differential inputs guide the development of domain-specificity in each network (17, 21–23). Specifically, face selectivity may be more likely to emerge in a network that receives disproportionate input from the fovea over development (and vice versa for scenes). However, despite widespread hypotheses about the importance of such a retinotopic “protoarchitecture,” little is known about how high-level visual cortex is connected to early visual cortex in the earliest stages of development—a crucial first step toward elucidating a potential role for connectivity in the development of domain-specific function. Although one study in newborn macaques found that the proto middle face patch shows stronger connectivity to the fovea than to the peripheral primary visual cortex (V1) (21), no study has tested whether similar results are found in human neonates, nor has any study examined connectivity between the scene-selective cortex and peripheral visual cortex in neonates. Thus, here we did just that by exploring functional connectivity between the proto face and scene networks and early visual cortex early in postnatal life.

Functional connectivity was assessed by measuring correlations of spontaneous BOLD fluctuations between pairs of regions while neonates (mean age, 27 d; range, 6 to 57 d) slept swaddled in the scanner, producing low-motion rsfMRI data. Regions of interest (ROIs) were identified using functional “parcels” based on a large sample of adult data (24), as described in *Methods* (Fig. 1). This parcel approach allowed us to independently

define proto face- and scene-selective regions of the neonate brain despite previous findings indicating that adult-like selectivity for faces and scenes (i.e., greater responses to faces or scenes than to objects) is not yet developed at this age, or even by age 4 to 6 mo (2). V1 was identified anatomically using the Juelich histological atlas (25) and was divided into three equal portions along the posterior-to-anterior axis, thus identifying the foveal, middle, and peripheral V1. Finally, as a reference group, we conducted the same analyses using the same methods in 15 healthy adults.

Results

The Proto Face and Scene Networks Show Domain-Specific Connectivity in Neonates. To validate our approach, we began by confirming that domain-specific functional connectivity could be detected in adults using the methods described above. If functional connectivity is domain-specific, then we should see stronger functional connectivity within domains (i.e., OFA-FFA and PPA-RSC) than between domains (i.e., any pair of a face and a scene region). To maximize statistical power, within-hemisphere (e.g., rOFA-rFFA) and between-hemisphere (e.g., rOFA-lFFA) correlations were averaged together for each pair of regions in each subject. (Note that between-hemisphere correlations did not include homotopic connections, such as rFFA-lFFA, and were also analyzed separately, as discussed below; Fig. 2C.) Indeed, in adults, we found significantly greater within-domain functional connectivity than between-domain functional connectivity (paired samples *t* test: $t_{(14)} = 9.26$, $P < 0.001$, $d = 2.39$) (Fig. 2A). Fifteen out of 15 adults showed this effect (i.e., numerically greater connectivity within domains than between domains). To further investigate this domain-specific effect and explore whether it is present in both face and scene networks individually, we conducted one-way repeated-measures ANOVA comparing all possible functional connections (i.e., OFA-FFA, PPA-RSC, OFA-PPA, FFA-PPA, OFA-RSC, FFA-RSC). This analysis revealed a significant main effect of connection ($F_{(5,70)} = 22.90$, $P < 0.001$, $\eta_p^2 = 0.62$), driven by stronger functional connectivity between OFA and FFA than any between-domain combination of a face and a scene region (pairwise comparisons, $P < 0.05$ for all), as well as by stronger connectivity between PPA and RSC than any between-domain combination of a face and a scene region (pairwise comparisons, $P < 0.001$ for all), replicating previous findings (6–8) (Fig. 2B). All pairwise comparisons also survived Bonferroni correction, with the exception of marginally significant effects for OFA-FFA vs. OFA-PPA ($P = 0.07$) and OFA-FFA vs. OFA-RSC ($P = 0.06$).

We next used the same approach to test for domain-specific functional connectivity in neonates. We found significantly greater within-domain than between-domain functional connectivity (paired-samples *t* test: $t_{(29)} = 6.14$, $P < 0.001$, $d = 1.12$) (Fig. 2A). Twenty-seven out of 30 neonates showed this effect (i.e., numerically greater connectivity within than between domains) (*SI Appendix*, Fig. S1A). To further investigate this domain-specific effect and explore whether it is present in both face and scene networks individually, we conducted a one-way repeated-measures ANOVA comparing all possible functional connections: OFA-FFA, PPA-RSC, OFA-PPA, FFA-PPA, OFA-RSC, and FFA-RSC. This analysis revealed a significant main effect of connection ($F_{(5,145)} = 6.57$, $P < 0.001$, $\eta_p^2 = 0.19$), driven by stronger functional connectivity between OFA and FFA than any between-domain combination of a face and a scene region ($P < 0.01$ for all, with the exception of FFA-PPA, the single shortest connection, where $P = 0.18$; see the discussion of distance confounds below), as well as stronger functional connectivity between PPA and RSC than any between-domain combination of a face and a scene region (pairwise comparisons, $P < 0.01$ for all, again with the exception of FFA-PPA, the single shortest connection, at $P = 0.17$) (Fig. 2B). This same pattern of results remained with Bonferroni-corrected pairwise comparisons ($P < 0.05$ for all, again with the exceptions of OFA-FFA vs. FFA-PPA,

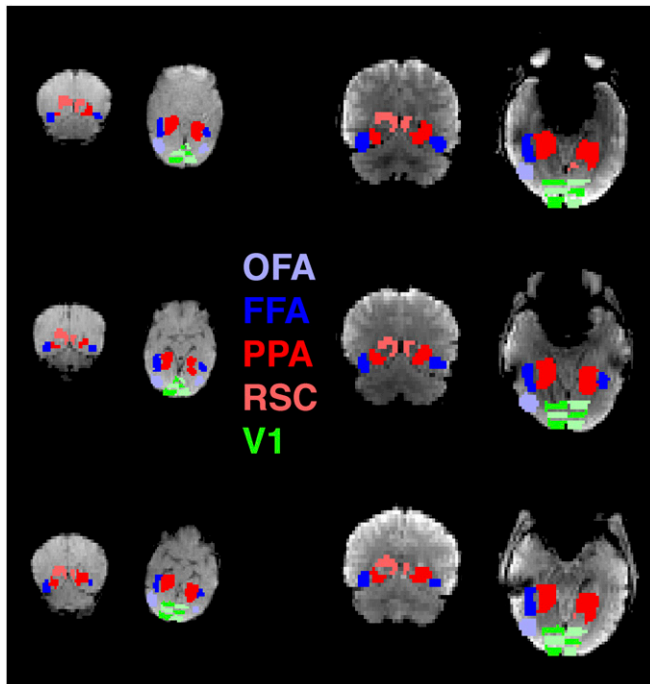


Fig. 1. ROIs of interest in three example neonates (*Left*) and three example adults (*Right*). OFA, light blue; FFA, dark blue; PPA, red; RSC, pink; V1, green. Note that V1 was split into three equal portions from posterior to anterior, as distinguished by alternating patterns of green and light green.

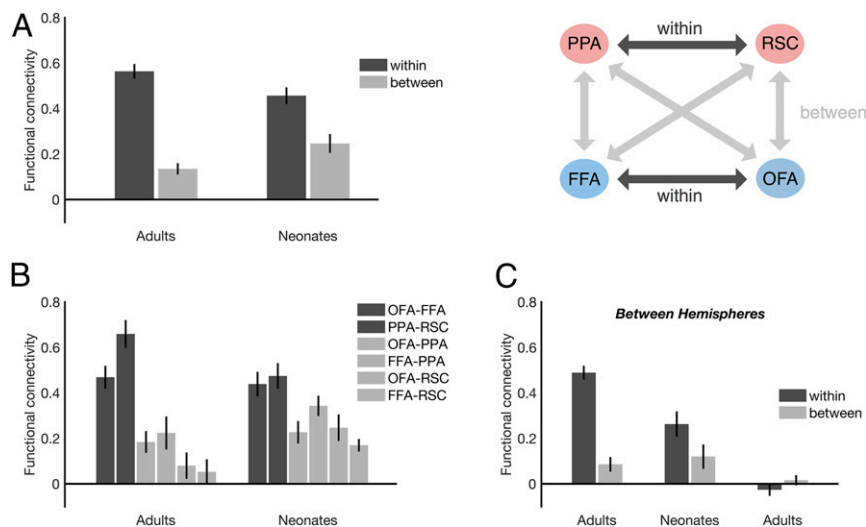


Fig. 2. Domain-specific functional connectivity in neonates and adults. (A) Both neonates ($n = 30$) and adults ($n = 15$) show greater functional connectivity within domains (i.e., OFA-FFA and PPA-RSC) than between domains (i.e., any pair of a face and a scene region). (B) Functional connectivity between every possible pair of regions in both neonates and adults. (C) Greater functional connectivity within domains than between domains is found even in the between-hemisphere data, ensuring that effects are not driven by local spread of the fMRI signal. Furthermore, domain-specific functional connectivity is not found in noise data designed to simulate distance effects (*Methods*). Error bars indicate SEM.

with $P = 1.00$, and PPA-RSC vs. FFA-PPA, with $P = 1.00$, the shortest connections). For further assessment of the strength and selectivity of within-network patterns, we also conducted a seed-based analysis of functional connectivity across the whole brain, which revealed qualitatively similar results to our ROI analysis (*SI Appendix, Fig. S2*). These results show that domain-specific functional connectivity is already present in the proto face and scene networks by age 27 d.

We next asked whether domain-specific functional connectivity develops from the first weeks of life to adulthood by comparing the neonates and adults directly. A two (group: adults, neonates) \times two (domain: within, between) mixed-model ANOVA revealed a significant main effect of domain ($F_{(1,43)} = 117.55$, $P = 0.001$, $\eta_p^2 = 0.73$), as well as a significant group \times domain interaction ($F_{(1,43)} = 13.00$, $P = 0.001$, $\eta_p^2 = 0.23$), with adults showing stronger domain-specific functional connectivity than neonates (Fig. 2A). These results are consistent with the idea that although neonates already show domain-specific functional connectivity by 27 d, the strength of this functional connectivity nevertheless increases from the first weeks of life to adulthood, consistent with previous evidence that OFA-FFA functional connectivity is still developing later in childhood (26–28).

Domain-Specific Functional Connectivity in Neonates Is Not Driven by Distance-Related Confounds, Instrumental Sampling, or Preprocessing.

Given that the two face regions are relatively close to one another in cortex and the two scene regions are also close to one another in cortex, it is possible the pattern of functional connectivity described above was driven by distance-related confounds (i.e., the intrinsic

spread of the fMRI signal), rather than by true functional connectivity per se. Indeed, when we measured the volumetric distances between each pair of regions, we found that within-domain connections were generally shorter than between-domain connections (average distance within, 19.09 mm; average distance between, 23.45 mm) (Table 1).

To rule out the possibility of local distance confounds, we separately investigated the between-hemisphere functional connectivity rather than the average of within- and between-hemisphere connectivity. Between-hemisphere connections are well beyond the range of the local spread of the fMRI signal and therefore control for distance-related confounds (even in the event that the relevant fMRI signal spread occurs along the cortical surface rather than across the volume). Importantly, again, homotopic connections (e.g., rFFA-IFFA) were excluded from the between-hemisphere analysis, ensuring that these connections could not bias within-domain connectivity. Here we still found significantly greater functional connectivity within domains compared with between domains for both neonates (paired-samples t test; $t_{(29)} = 3.56$, $P < 0.001$, $d = 0.69$) and adults ($t_{(14)} = 8.93$, $P < 0.001$, $d = 2.31$), as well as a significant group (neonates, adults) \times domain (within, between) interaction ($F_{(1,43)} = 13.72$, $P = 0.001$, $\eta_p^2 = 0.24$, mixed-model ANOVA) (Fig. 2C).

To further confirm this result, and also rule out the possibility that our results could be attributed to biases in instrumental sampling or preprocessing, we generated noise data (i.e., data in which no reliable functional connectivity could possibly be found; *Methods*) that were smoothed to mimic the intrinsic spread of the fMRI signal (and therefore any such distance

Table 1. Volumetric distances (in mm) between pairs of regions testing domain-specific functional connectivity

Group	Within domains	Between domains	OFA-FFA	PPA-RSC	OFA-PPA	FFA-PPA	OFA-RSC	FFA-RSC
Neonates								
Within hemispheres	19.09	23.45	18.90	19.28	24.70	14.44	26.03	28.63
Between hemispheres	46.06	45.68	59.60	32.52	49.22	46.64	42.04	44.83
Adults								
Within hemispheres	23.86	31.34	24.66	23.06	33.67	19.39	35.96	36.33
Between hemispheres	62.89	63.05	82.59	43.19	68.87	65.21	58.24	59.88

effects), and passed these data through the same processing pipeline used to analyze the real data. These noise data failed to show a domain-specific effect between hemispheres (paired-samples t test; $t_{(29)} = 1.52$, $P = 0.14$, $d = 0.28$), and produced correlations that were not reliably different from zero (Fig. 2C). Moreover, directly comparing the neonate and noise data, a two (group: neonates, noise) \times two (domain: within, between) mixed-model ANOVA revealed a significant group \times domain interaction ($F_{(1,58)} = 13.88$, $P < 0.001$, $\eta_p^2 = 1.93$). Therefore, our findings cannot be explained by distance-related confounds.

The Proto Face and Scene Networks Show Biased Connectivity with Foveal and Peripheral V1. The foregoing findings suggest that the face and scene networks show domain-specific patterns of functional connectivity in the earliest days of life. But do these networks further show differential connectivity with early visual cortex, as is found in adulthood? Addressing this question, we next asked whether the proto face network shows biased connectivity with foveal V1, while the proto scene network shows biased connectivity with peripheral V1. To validate our approach, we began by asking whether the face network in adults shows stronger connectivity with foveal V1 than with peripheral V1, while the scene network shows the opposite pattern. Again, to maximize statistical power, within-hemisphere (e.g., rOFA-rV1) and between-hemisphere (e.g., rOFA-IV1) correlations were averaged together for each pair of regions in each subject. (Between-hemisphere correlations were also analyzed separately and are discussed below; Fig. 3 C and D.) Before the statistical analysis, we created an eccentricity bias metric by averaging “within-eccentricity” conditions (i.e., both OFA and FFA connecting to foveal V1 and both PPA and RSC connecting to peripheral V1) and “between-eccentricity” conditions (i.e., both OFA and FFA connecting to peripheral V1 and both PPA and RSC connecting to foveal V1). Note that the “middle” V1 ROI was not used in calculating this eccentricity bias metric, since the “middle” V1 ROI is neither within nor between eccentricity, although we still investigated it, as discussed below. Indeed, for

adults, we found significantly stronger connectivity within eccentricity than between eccentricity (paired-samples t test; $t_{(14)} = 8.06$, $P < 0.001$, $d = 2.08$) (Fig. 3A). Fifteen out of 15 adults showed this effect (i.e., numerically greater connectivity within eccentricity than between eccentricity).

To further investigate the nature of this effect, we next analyzed each face and scene region individually (Fig. 3B), exploring the pattern of functional connectivity of each region across all three portions of V1 (foveal, middle, and peripheral). For the face regions, we found a significant linear trend in OFA ($F_{(1,14)} = 5.49$, $p = 0.03$, $\eta_p^2 = 0.28$), reflecting decreasing connectivity from foveal to middle to peripheral V1, but not in FFA ($F_{(1,14)} = 1.59$, $p = 0.23$, $\eta_p^2 = 0.10$), although there was a numerical trend in the direction of a foveal bias. The failure to observe a significant foveal bias for FFA alone is consistent with a previous study measuring connectivity between foveal V1 and FFA in humans that likewise did not find a strong foveal bias in FFA (18). Indeed, it is possible that more sensitive methods are needed to detect this effect (e.g., ref. 21). In contrast, for the scene regions, we found significant linear trends in PPA ($F_{(1,14)} = 52.06$, $P < 0.001$, $\eta_p^2 = 0.79$) and RSC ($F_{(1,14)} = 58.93$, $P < 0.001$, $\eta_p^2 = 0.81$), with both scene regions showing increasing connectivity from foveal to middle to peripheral V1.

We next used the same approach to test for eccentricity-biased functional connectivity in neonates. Strikingly, we found significantly stronger connectivity within eccentricity than between eccentricity (paired-samples t test; $t_{(29)} = 5.19$, $P < 0.001$, $d = 0.95$) (Fig. 3A). Twenty-seven out of 30 neonates showed this effect (i.e., numerically greater connectivity within eccentricity than between eccentricity) (SI Appendix, Fig. S1B). To further investigate the nature of this effect, we next analyzed each face and scene region individually, exploring the pattern of functional connectivity of each region across all three portions of V1 (foveal, middle, and peripheral) (Fig. 3B). For the face regions, we found a significant linear trend in OFA ($F_{(1,29)} = 12.42$, $P = 0.001$, $\eta_p^2 = 0.30$), reflecting decreasing connectivity from foveal to middle to peripheral V1, but not in FFA ($F_{(1,29)} = 0.88$, $P = 0.36$, $\eta_p^2 = 0.03$),

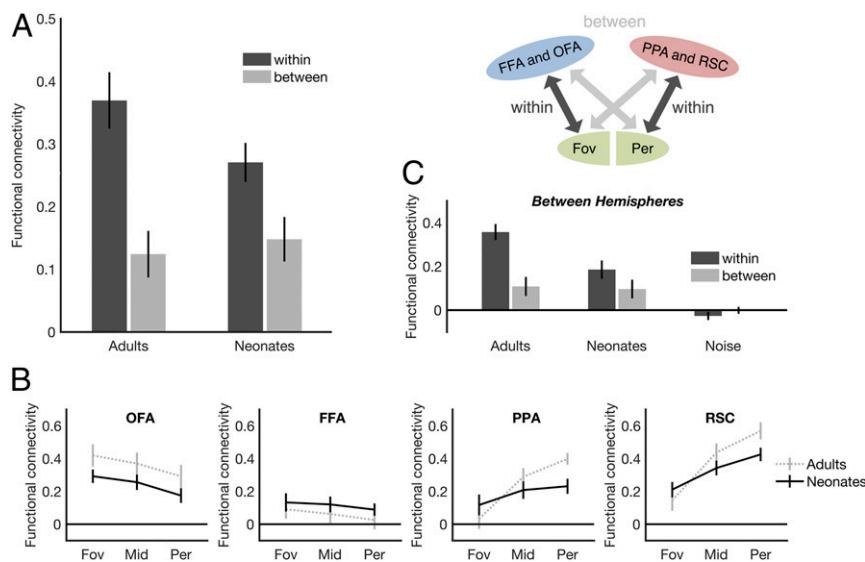


Fig. 3. Eccentricity-biased functional connectivity in neonates and adults. (A) Both neonates ($n = 30$) and adults ($n = 15$) show greater functional connectivity within eccentricity (i.e., face regions to foveal V1 and scene regions to peripheral V1) than between eccentricity (i.e., face regions to peripheral V1 or scene regions to foveal V1). Eccentricity-biased functional connectivity is not found in noise data designed to simulate distance effects (Methods). (B) Functional connectivity between each face (OFA and FFA) and place (PPA and RSC) region and the three portions of V1, representing foveal (“fov”), middle (“mid”), and peripheral (“per”) V1. (C) Greater functional connectivity within eccentricity than between eccentricity is found even in the between-hemisphere data, ensuring that effects are not driven by local spread of the fMRI signal. Furthermore, domain-specific functional connectivity is not found in noise data designed to simulate distance effects (Methods). Error bars indicate SEM.

although there was a numerical trend in the direction of a foveal bias, similar to the pattern seen in the adult data. Also similar to the adult findings, we found a significant linear trend in PPA ($F_{(1,29)} = 4.03$, $P = 0.05$, $\eta_p^2 = 0.12$) and in RSC ($F_{(1,29)} = 20.48$, $P < 0.001$, $\eta_p^2 = 0.41$), with both scene regions showing increasing connectivity from foveal to middle to peripheral V1. Taken together, these findings reveal initial evidence that the proto face and scene networks already show biased connectivity with foveal and peripheral early visual cortex, respectively, by age 27 d—at least in the cases of OFA, PPA, and RSC.

We next asked whether the eccentricity biases of the face and scene networks are still developing by comparing neonates and adults directly. A two (group: neonates, adults) \times two (eccentricity: within, between) mixed-model ANOVA revealed a significant main effect of eccentricity ($F_{(1,43)} = 85.64$, $P = 0.001$, $\eta_p^2 = 0.67$), as well as a significant group \times eccentricity interaction ($F_{(1,43)} = 9.52$, $P = 0.004$, $\eta_p^2 = 0.18$), with adults showing stronger eccentricity-biased functional connectivity than neonates. This finding is consistent with previous findings that eccentricity biases in high-level visual cortex are still developing later in childhood (29) and suggests that although eccentricity-biased functional connectivity may be qualitatively present as soon as 27 d of life, it continues to develop from infancy to adulthood.

Eccentricity-Biased Functional Connectivity in Neonates Is Not Driven by Distance-Related Confounds, Instrumental Sampling, or Preprocessing.

The eccentricity-biased connectivity cannot be explained by distance-related confounds (i.e., the intrinsic spread of the fMRI signal). Indeed, when we measured the volumetric distances between each face and scene region and V1, we found all four regions were closer to peripheral V1 than to foveal V1 (Table 2). Nevertheless, to ensure that local distance confounds could not possibly explain our results, we investigated the between-hemisphere functional connectivity alone, well beyond the range of the local spread of the fMRI signal. Here we still found significantly stronger connectivity within eccentricity than between eccentricity for neonates (paired-samples t test; $t_{(29)} = 3.57$, $P < 0.001$, $d = 0.65$) and adults ($t_{(14)} = 8.00$, $P < 0.001$, $d = 2.07$), as well as a significant group (neonates, adults) \times eccentricity (within, between) interaction ($F_{(1,43)} = 14.76$, $P = 0.001$, $\eta_p^2 = 0.26$; mixed-model ANOVA) (Fig. 3C). Moreover, noise data failed to show a eccentricity-bias effect between hemispheres (paired-samples t test; $t_{(29)} = 1.09$, $P = 0.28$, $d = 0.20$), producing correlations that were not reliably different from zero (Fig. 3C). Thus, our findings cannot be explained by distance-related confounds, instrumental sampling, or preprocessing and instead reflect initial evidence of eccentricity-biased functional connectivity of the proto face and scene networks toward foveal and peripheral V1, respectively.

Domain-Specific Functional Connectivity Is Not Driven by Eccentricity-Biased Functional Connectivity.

The finding that the face and scene networks may be biased toward foveal and peripheral input, respectively, raises the possibility that regions within each network are not truly functionally connected to one another, but rather show functional correlations due simply to a common source of input; for example, PPA and RSC may appear to be functionally connected simply because they are both connected to peripheral V1. Therefore, we performed partial correlation analyses, which allowed us to assess domain-specific functional connectivity while holding V1 constant. Specifically, OFA-FFA functional connectivity was recalculated after partialling out the time course from foveal V1, while PPA-RSC functional connectivity was recalculated after partialling out the time course from peripheral V1. This partial correlation analysis still revealed greater within-domain than between-domain connectivity in both neonates (paired-samples t test; $t_{(29)} = 5.80$, $P < 0.001$, $d = 1.06$) and adults ($t_{(14)} = 9.94$, $P < 0.001$, $d = 2.57$). Thus, domain-specific connectivity in the face and scene networks does not simply reflect common information inherited from regions earlier in the cortical processing hierarchy.

Importantly, it was previously hypothesized that the visual system contains an innate, retinotopic proto-organization in which domain-specific systems are organized in cortex based on retinotopic biases alone (21, 22, but see refs. 30–32). While our finding of eccentricity-biased functional connectivity in 27-d-old neonates supports this hypothesis, our present results go further to suggest that the innate proto-organization of the visual system is not merely retinotopic, but also includes domain-specific connections.

Discussion

Here we report the earliest examination of the cortical face- and scene-processing networks performed to date, revealing domain-specific functional connectivity in the proto face and scene networks as early as 27 d of age. The face and scene networks further showed evidence of biased functional connectivity to different portions of primary visual cortex, with face regions showing biased connectivity to foveal V1 and scene regions showing biased connectivity to peripheral V1. Thus, connectivity underlying the cortical face and scene networks is strikingly early developing, if not innate.

The present findings provide empirical support in humans for the hypothesis that connectivity precedes function in the developing cortex (33), showing that connectivity underlying the cortical face and scene processing networks is already present within the first few weeks of postnatal life—months earlier than domain-specific function emerges in these networks, based on

Table 2. Volumetric distances (in mm) between pairs of regions testing eccentricity-biased functional connectivity

Group	Within hemispheres			Between hemispheres		
	Foveal V1	Middle V1	Peripheral V1	Foveal V1	Middle V1	Peripheral V1
OFA						
Neonates	23.89	23.30	21.84	39.30	35.22	35.60
Adults	33.79	32.88	31.61	55.57	49.65	49.79
FFA						
Neonates	39.37	36.04	31.52	50.94	45.31	42.92
Adults	54.16	49.08	43.31	70.77	62.36	58.79
PPA						
Neonates	37.92	32.04	25.82	45.23	38.30	34.03
Adults	52.49	43.77	35.32	63.04	52.79	46.61
RSC						
Neonates	28.34	20.48	13.54	33.89	25.88	21.47
Adults	39.78	28.62	18.48	47.72	36.25	29.41

converging evidence from infant humans and macaques (2, 3). The finding that domain-specific connectivity is already intact in the earliest days of life suggests a role for these connections in shaping later development (e.g., by ensuring that regions within a network go on to develop similar functions, independent of regions in other networks). Nevertheless, factors beyond connectivity may contribute to the development of the face and scene networks as well. For example, by adulthood, face and scene regions show different cytoarchitectural profiles (34), raising the possibility that intrinsic, anatomic properties of the cortical regions themselves within each network also constrain subsequent development.

But why is it that one network always develops selectivity for face processing in particular while the other network always develops selectivity for scene processing, and never the other way around? Although our study cannot answer this question directly, our finding that the proto face and scene processing networks show eccentricity-biased functional connectivity by age 27 d is consistent with at least two hypotheses. One of these hypotheses is that early-emerging, eccentricity-biased connectivity is sufficient on its own to drive the functional dissociation between these networks (22). In particular, given that faces are typically foveated, even from the earliest days of life (35, 36), while scenes inherently extend across the entire visual field, face selectivity may emerge in the network that receives disproportionate stimulation from the fovea (and, consequently, faces), while scene selectivity may emerge in the network that receives disproportionate stimulation from the periphery (and, consequently, scenes). This hypothesis is appealing in that it readily predicts the current finding that eccentricity-biased functional connectivity is established before the development of full-fledged domain-specific function in these networks. However, faces are not the only stimulus that we foveate, and both face- and scene-selective responses have been found in the congenitally blind (i.e., in the complete absence of structured bottom-up visual input during development) (37, 38), suggesting that bottom-up connections alone are insufficient to explain how domain-specific function develops (31). Indeed, it has been recently proposed that the development of domain-specific function depends on other connections beyond those from early visual cortex, such as top-down connections from early-developing regions involved in contingent social interactions (in the case of the face network), including the medial prefrontal cortex (30). Likewise, given that scene-selective cortex in adulthood shows connectivity with regions involved in navigation and spatial cognition, including the hippocampus and parietal cortex (39), it is possible that top-down connections could scaffold the development of scene selectivity in this network as well.

In contrast, a second hypothesis is that the eccentricity-biased functional connectivity may develop in anticipation of domain-specific function in each network to facilitate domain-specific processing after that function develops or even may help refine the development of domain-specific function in each network in concert with other constraints (e.g., top-down connections, cytoarchitecture), essentially combining the first and second hypotheses. Indeed, while face- and scene-selective responses are observed in congenitally blind adults, it remains unclear whether the selectivity of responses in those systems is equal to that in sighted individuals, suggesting that bottom-up input may still play some role in development. Clearly then, future work is needed to identify the precise role of eccentricity-biased connectivity in development and, more broadly, to determine how each network always takes on its own particular domain-specific function.

In conclusion, the present findings reveal that domain-specific patterns of functional connectivity are present in human cortex by just 27 d of age and, further, that these proto domain-specific networks already receive differential visual inputs. Our results

therefore support the hypothesis that connectivity precedes function in the developing cortex and suggest that the human brain does not begin as a relatively undifferentiated, general-purpose machine, but rather comes prewired with particular networks already in place, setting the stage for later development.

Methods

Participants. Thirty three neonates (mean age, 27 d; SD, 13 d; range, 6 to 57 d; 17 females) and 15 adults (mean age, 27.38 y; SD, 4.85 y; range, 21.46 to 38.83 y; 7 females) completed the study. Three neonates (2 females) were removed from the analyses due to excessive motion (i.e., >2 mm absolute mean frame-wise displacement), resulting in a final sample of 30 neonates. No adult participants were excluded. Study procedures were approved by the Emory University Institutional Review Board, and all participants or parents of participants provided written consent before scanning.

MRI Acquisition. Scanning was performed on a 3-T Siemens scanner, either at Children's Healthcare of Atlanta Egleston Hospital (CHOA) (neonates only, $n = 20$) or at the Facility for Education and Research in Neuroscience (FERN) (neonates, $n = 10$; all adults) at Emory University. All functional images were acquired using a standard 32-channel head matrix coil and a gradient-echo single-shot echo planar imaging sequence (neonate scans conducted at CHOA: repetition time [TR] = 2,000 ms, echo time [TE] = 30, acquisition matrix = $92 \times 92 \times 34$, and voxel size = $2.391 \times 2.391 \times 5 \text{ mm}^3$; neonate scans conducted at FERN: TR = 1,000 ms, TE = 30, acquisition matrix = $72 \times 72 \times 39$, and voxel size = $2.5 \times 2.5 \times 2.5 \text{ mm}^3$; adult scan sequence 1 [$n = 11$]: TR = 2,000 ms, TE = 30, acquisition matrix = $128 \times 128 \times 28$, and voxel size = $1.5 \times 1.5 \times 2.5 \text{ mm}^3$; adult scan sequence 2 [$n = 4$]: TR = 2,000 ms, TE = 30, acquisition matrix = $64 \times 64 \times 35$, and voxel size = $3.1 \times 3.1 \times 4.4 \text{ mm}^3$). For scans conducted at CHOA, neonates completed one run of 130 volumes. For scans conducted at FERN, neonates completed one to four runs of 300 volumes each. Functional connectivity for each cohort separately is shown in *SI Appendix, Fig. S3*. Before scanning, all neonates were swaddled and encouraged to sleep (e.g., via rocking, feeding). Neonates were fitted with earplugs and earmuffs to reduce exposure to scanner noise and then placed in a MedVac neonate immobilizer to reduce movement during scanning procedures. Adults were instructed to simply lie still and awake with their eyes open, thinking of nothing in particular. In addition, in all participants, a higher-resolution anatomic scan was collected for registration purposes.

Image Preprocessing and Data Analysis. Functional data were analyzed with FSL 5.0.11. The preprocessing consisted of motion correction, detrending, slice time correction, intensity normalization, and spatial smoothing (Gaussian kernel, 8 mm FWHM). Images were bandpass-filtered (0.01 to 0.08 Hz) to retain low-frequency signal only, and several sources of nuisance variance were removed via regression, including six motion parameter estimates and the mean signal from a ventricular and white matter region.

ROI Selection. ROIs were defined using an atlas of functional "parcels" (24) that identify the anatomic regions within which most subjects show activation for the contrast of faces minus objects (for OFA and FFA) or scenes minus objects (for PPA and RSC). Parcels were registered from standard space to each subject's functional space using the FSL linear registration tool, and overlapping voxels for any pair of parcels were removed from those ROIs. To validate the registration of the functional parcels to each neonate's brain (which involved transformation from adult standard space to neonate functional space), we also registered functional data from a group of 5-month infants (representing a group contrast of faces > scenes; taken from ref. 2) to each neonate's brain (thus involving an independent transformation from infant group space to neonate functional space) and found consistent localization of OFA, FFA, PPA, and RSC across the two methods. To quantify the consistency of this localization, we extracted the mean t value from the group contrast map in each ROI and found that both OFA and FFA showed positive t values, indicating stronger responses to faces than scenes (OFA, $t = 0.67$; FFA, $t = 0.77$) while both PPA and RSC showed negative t values, indicating stronger responses to scenes than to faces (PPA, $t = -1.96$; RSC, $t = -0.25$).

Resting-State Correlation. After preprocessing, a continuous time course for each ROI was extracted by averaging the time courses of all voxels within the ROI. Thus, we obtained a time course consisting of 130 to 300 data points for each ROI, participant, and run (where applicable). Temporal correlation coefficients between the extracted time course from a given ROI and those from other ROIs were calculated to determine which regions were functionally correlated at rest. Correlation coefficients (r) were transformed to

Gaussian-distributed z-scores via Fisher's transformation to improve normality, and these z-scores were then used for further analyses (8, 40).

Noise Data Analysis. To test whether our findings might be explained by the intrinsic spread of the fMRI signal, we generated noise data (in which no significant correlations should be found) that were smoothed to approximately match the spatial resolution of the BOLD signal and thus any distance-related effects. Specifically, the time course of each voxel in each neonate's raw dataset was replaced with a random time course with the same temporal signal-to-noise ratio (i.e., the same mean signal strength and variability) found in that voxel in the real neonate data. These noise data were then smoothed with a 3.5-mm Gaussian kernel, mimicking the approximate spatial resolution of the BOLD signal (i.e., 3.5 mm) (21, 41). The resultant smoothed noise data were then submitted to exactly the same processing stream used to analyze the real neonate data, including the same spatial smoothing we applied to the real neonate data.

1. N. Kanwisher, D. Dilks, "The functional organization of the ventral visual pathway in humans" in *The New Visual Neurosciences*, L. Chalupa, J. Werner, Eds. (MIT Press, Cambridge, MA, 2013), pp. 733–748.
2. B. Deen *et al.*, Organization of high-level visual cortex in human infants. *Nat. Commun.* **8**, 13995 (2017).
3. M. S. Livingstone *et al.*, Development of the macaque face-patch system. *Nat. Commun.* **8**, 14897 (2017).
4. M. Gschwind, G. Pourtois, S. Schwartz, D. Van De Ville, P. Vuilleumier, White-matter connectivity between face-responsive regions in the human brain. *Cereb. Cortex* **22**, 1564–1576 (2012).
5. J. A. Pyles, T. D. Verstynen, W. Schneider, M. J. Tarr, Explicating the face perception network with white matter connectivity. *PLoS One* **8**, e61611 (2013).
6. Y. Nir, U. Hasson, I. Levy, Y. Yeshurun, R. Malach, Widespread functional connectivity and fMRI fluctuations in human visual cortex in the absence of visual stimulation. *Neuroimage* **30**, 1313–1324 (2006).
7. H. Zhang, J. Tian, J. Liu, J. Li, K. Lee, Intrinsically organized network for face perception during the resting state. *Neurosci. Lett.* **454**, 1–5 (2009).
8. Q. Zhu, J. Zhang, Y. L. Luo, D. D. Dilks, J. Liu, Resting-state neural activity across face-selective cortical regions is behaviorally relevant. *J. Neurosci.* **31**, 10323–10330 (2011).
9. D. Pitcher, B. Duchaine, V. Walsh, Combined TMS and fMRI reveal dissociable cortical pathways for dynamic and static face perception. *Curr. Biol.* **24**, 2066–2070 (2014).
10. W. D. Stevens, M. H. Tessler, C. S. Peng, A. Martin, Functional connectivity constrains the category-related organization of human ventral occipitotemporal cortex. *Hum. Brain Mapp.* **36**, 2187–2206 (2015).
11. B. Z. Mahon, A. Caramazza, What drives the organization of object knowledge in the brain? *Trends Cogn. Sci.* **15**, 97–103 (2011).
12. M. Riesenhuber, Appearance isn't everything: News on object representation in cortex. *Neuron* **55**, 341–344 (2007).
13. Q. Chen, F. E. Garcea, J. Almeida, B. Z. Mahon, Connectivity-based constraints on category-specificity in the ventral object processing pathway. *Neuropsychologia* **105**, 184–196 (2017).
14. R. M. Hutchison, J. C. Culham, S. Everling, J. R. Flanagan, J. P. Gallivan, Distinct and distributed functional connectivity patterns across cortex reflect the domain-specific constraints of object, face, scene, body, and tool category-selective modules in the ventral visual pathway. *Neuroimage* **96**, 216–236 (2014).
15. T. Konkle, A. Caramazza, The large-scale organization of object-responsive cortex is reflected in resting-state network architecture. *Cereb. Cortex* **27**, 4933–4945 (2017).
16. U. Hasson, I. Levy, M. Behrmann, T. Hendler, R. Malach, Eccentricity bias as an organizing principle for human high-order object areas. *Neuron* **34**, 479–490 (2002).
17. I. Levy, U. Hasson, G. Avidan, T. Hendler, R. Malach, Center-periphery organization of human object areas. *Nat. Neurosci.* **4**, 533–539 (2001).
18. E. Striem-Amit *et al.*, Functional connectivity of visual cortex in the blind follows retinotopic organization principles. *Brain* **138**, 1679–1695 (2015).
19. P. Mäkelä, R. Näsänen, J. Rovamo, D. Melmoth, Identification of facial images in peripheral vision. *Vision Res.* **41**, 599–610 (2001).
20. A. M. Larson, L. C. Loschky, The contributions of central versus peripheral vision to scene gist recognition. *J. Vision* **9**, 6.1–16 (2009).
21. M. J. Arcaro, M. S. Livingstone, A hierarchical, retinotopic proto-organization of the primate visual system at birth. *eLife* **6**, e26196 (2017).

Data and Materials Availability. The datasets generated during this study are available at <https://osf.io/kmxv7/>.

ACKNOWLEDGMENTS. We thank the Facility for Education and Research in Neuroscience Imaging Center in the Department of Psychology, Emory University, Atlanta, GA, as well as the Children's Healthcare of Atlanta Egleston Hospital. We also thank Nancy Kanwisher, Philippe Rochat, Mike McCloskey, and Barbara Landau for insightful comments, as well as Katrina C. Johnson for help with data collection. This work was supported by Emory College, Emory University (D.D.D.), the National Eye Institute (Grant R01 EY029724, to D.D.D.), the Emory University HERCULES Exposome Research Center (Grant NIEHS P30 ES019776, to D.D.D.), the National Eye Institute (Grant T32EY7092, to F.S.K.), the NSF Graduate Research Fellowship Program (Grant DGE-1444932, to C.L.H.), an Eleanor Munsterberg Koppitz Dissertation Fellowship (to C.L.H.), and a National Alliance for Research on Schizophrenia & Depression Young Investigator Award (to Katrina C. Johnson).

22. M. S. Livingstone, M. J. Arcaro, P. F. Schade, Cortex is cortex: Ubiquitous principles drive face-domain development. *Trends Cogn. Sci.* **23**, 3–4 (2019).
23. M. J. Arcaro, P. F. Schade, M. S. Livingstone, Universal mechanisms and the development of the face network: What you see is what you get. *Annu. Rev. Vis. Sci.* **5**, 341–372 (2019).
24. J. B. Julian, E. Fedorenko, J. Webster, N. Kanwisher, An algorithmic method for functionally defining regions of interest in the ventral visual pathway. *Neuroimage* **60**, 2357–2364 (2012).
25. K. Amunts, A. Malikovic, H. Mohlberg, T. Schormann, K. Zilles, Brodmann's areas 17 and 18 brought into stereotaxic space—where and how variable? *Neuroimage* **11**, 66–84 (2000).
26. Y. Song, Q. Zhu, J. Li, X. Wang, J. Liu, Typical and atypical development of functional connectivity in the face network. *J. Neurosci.* **35**, 14624–14635 (2015).
27. K. Cohen Kadosh, R. Cohen Kadosh, F. Dick, M. H. Johnson, Developmental changes in effective connectivity in the emerging core face network. *Cereb. Cortex* **21**, 1389–1394 (2011).
28. J. E. Joseph *et al.*, The changing landscape of functional brain networks for face processing in typical development. *Neuroimage* **63**, 1223–1236 (2012).
29. J. Gomez, V. Natu, B. Jeska, M. Barnett, K. Grill-Spector, Development differentially sculpts receptive fields across early and high-level human visual cortex. *Nat. Commun.* **9**, 788 (2018).
30. L. J. Powell, H. L. Kosakowski, R. Saxe, Social origins of cortical face areas. *Trends Cogn. Sci.* **22**, 752–763 (2018).
31. H. P. Op de Beeck, I. Pillet, J. B. Ritchie, Factors determining where category-selective areas emerge in visual cortex. *Trends Cogn. Sci.* **23**, 784–797 (2019).
32. B. Z. Mahon, S. Anzellotti, J. Schwarzbach, M. Zampini, A. Caramazza, Category-specific organization in the human brain does not require visual experience. *Neuron* **63**, 397–405 (2009).
33. Z. M. Saygin *et al.*, Connectivity precedes function in the development of the visual word form area. *Nat. Neurosci.* **19**, 1250–1255 (2016).
34. K. S. Weiner *et al.*, The cytoarchitecture of domain-specific regions in human high-level visual cortex. *Cereb. Cortex* **27**, 146–161 (2017).
35. S. Jayaraman, C. M. Fausey, L. B. Smith, Why are faces denser in the visual experiences of younger than older infants? *Dev. Psychol.* **53**, 38–49 (2017).
36. S. Jayaraman, C. M. Fausey, L. B. Smith, The faces in infant-perspective scenes change over the first year of life. *PLoS One* **10**, e0123780 (2015).
37. J. van den Hurk, M. Van Baelen, H. P. Op de Beeck, Development of visual category selectivity in ventral visual cortex does not require visual experience. *Proc. Natl. Acad. Sci. U.S.A.* **114**, E4501–E4510 (2017).
38. S. L. Fairhall *et al.*, Plastic reorganization of neural systems for perception of others in the congenitally blind. *Neuroimage* **158**, 126–135 (2017).
39. C. Baldassano, D. M. Beck, L. Fei-Fei, Differential connectivity within the parahippocampal place area. *Neuroimage* **75**, 228–237 (2013).
40. M. D. Fox, M. Corbetta, A. Z. Snyder, J. L. Vincent, M. E. Raichle, Spontaneous neuronal activity distinguishes human dorsal and ventral attention systems. *Proc. Natl. Acad. Sci. U.S.A.* **103**, 10046–10051 (2006).
41. S. M. Smirnakis *et al.*, Spatial specificity of BOLD versus cerebral blood volume fMRI for mapping cortical organization. *J. Cereb. Blood Flow Metab.* **27**, 1248–1261 (2007).